

Evidence for RNA in the Peptidyl Transferase Center of *Escherichia coli* Ribosomes As Indicated by Fluorescence†

William D. Picking,† O. W. Odom, and Boyd Hardesty*

Departments of Chemistry and Biochemistry and Clayton Foundation Biochemical Institute,
The University of Texas at Austin, Austin, Texas 78712

Received July 8, 1992; Revised Manuscript Received October 13, 1992

ABSTRACT: A coumarin derivative was covalently attached to either the amino acid or the 5' end of phenylalanine-specific transfer RNA (tRNA^{Phe}). Its fluorescence was quenched by methyl viologen when the tRNA was free in solution or bound to *Escherichia coli* ribosomes. Methyl viologen as a cation in solution has a strong affinity for the ionized phosphates of a nucleic acid and so can be used to qualitatively measure the presence of RNA in the immediate vicinity of the tRNA-linked coumarins upon binding to ribosomes. Fluorescence lifetime measurements indicate that the increase in fluorescence quenching observed when the tRNAs are bound into the peptidyl site of ribosomes is due to static quenching by methyl viologen bound to RNA in the immediate vicinity of the fluorophore. The data lead to the conclusion that the ribosome peptidyl transferase center is rich in ribosomal RNA. Movement of the fluorophore at the N-terminus of the nascent peptide as it is extended or movement of the tRNA acceptor stem away from the peptidyl transferase center during peptide bond formation appears to result in movement of the probe into a region containing less rRNA.

In early ribosome research, it was generally assumed that ribosomal proteins would have a key function and that ribosomal RNA (rRNA) would serve as the scaffold upon which these proteins were held in place (Fellner, 1974). Later, rRNA was postulated to be directly involved in ribosomal function with profound implications for the nature of very early self-replicating forms and evolution (Noller & Woese, 1981). To date, no catalytic function has been definitively attributed to any ribosomal protein. We have suggested that the ribosome as a functional entity may serve to align aminoacyl-tRNA and peptidyl-tRNA molecules so that peptide bond formation can take place by a displacement reaction without direct mediation of a protein catalytic center (Hardesty et al., 1986). These considerations have been extended to further arguments that rRNA is the key functional component of ribosomes (Raue et al., 1990; Noller, 1991).

Several segments of rRNA have been directly implicated in ribosome function, including elongation factor G and elongation factor Tu binding to 23S rRNA (Thompson et al., 1982; Skold, 1983; Moazed et al., 1988), antibiotic association with 16S rRNA (Moazed & Noller, 1987a) and 23S rRNA (Moazed & Noller, 1987b), antibiotic resistance with 23S rRNA (Cundliffe, 1986), mRNA binding (Shine & Dalgarno, 1974), and tRNA interaction with 23S rRNA and 16S rRNA (Schwartz & Ofengand, 1978; Barta et al., 1984; Moazed & Noller, 1990). Many of the rRNA segments which interact with these and other translational components are single-stranded regions such as those in domain V of the 23S rRNA which have been implicated as part of the peptidyl transferase center, the site at which peptide bond formation occurs (Noller, 1991).

We have used fluorescence techniques to examine a number of structural and functional features of *Escherichia coli* ribosomes with fluorophores covalently attached to specific sites on tRNAs, ribosomal proteins, or mRNA (Odom et al., 1990; Picking et al., 1992; Czerwowski et al., 1991; Hardesty et al., 1992). During the course of these studies, we have developed a method to qualitatively assess changes in the relative amount of nucleic acid in the immediate vicinity of a fluorescent probe covalently attached to free and ribosome-bound tRNA^{Phe} analogues. The method is based on the observation that methyl viologen (MV²⁺)¹ binds tightly to DNA ($K_a = 1.8 \times 10^5 \text{ M}^{-1}$) (Fromherz & Reiger, 1986), which greatly enhances its efficiency to quench fluorescence from probes such as ethidium bromide that are intercalated into double-stranded DNA (Atherton, 1988). The mechanism of quenching most likely involves photoinduced electron transfer from the coumarin excited singlet state. Although the process does not involve actual complex formation between fluorophore and quencher, the quenching behaves in typically static fashion in that the lifetime of the ethidium bromide remains constant (Atherton, 1988). MV²⁺ also quenches coumarin fluorescence by an electron-transfer mechanism (Jones et al., 1984).

The change in MV²⁺ quenching of fluorescence from coumarin attached to phenylalanine of Phe-tRNA upon binding to the ribosomal P site was studied. Fluorescence lifetime measurements indicate that the large increase in quenching that is observed is primarily due to static quenching

† This work was supported by grants to B.H. from the National Science Foundation (DMB-9018260) and from the Foundation for Research.

* To whom correspondence should be addressed at the Department of Chemistry, The University of Texas at Austin. Telephone: 512-471-5874. Fax: 512-471-8696.

† Present address: Department of Biology, Saint Louis University, St. Louis, MO 63103.

¹ Abbreviations: MV²⁺, methyl viologen (1,1'-dimethyl-4,4'-bipyridinium dichloride); CPM, 3-(4-maleimidophenyl)-7-diethylamino-4-methylcoumarin; CITC, 3-(4-isothiocyanatophenyl)-7-diethylamino-4-methylcoumarin; 5'-CITC-tRNA^{Phe}, yeast tRNA^{Phe} labeled at its 5' end with CITC; 5'-CITC-NAC-Phe-tRNA, yeast 5'-CITC-tRNA^{Phe} aminoacylated with phenylalanine, which was then acetylated at its α -amino group; CPM-SAC-Phe-tRNA, yeast tRNA^{Phe} aminoacylated with phenylalanine which was then mercaptoacetylated at its α -amino group and labeled with CPM; poly(Phe), polyphenylalanine; poly(Ala), polyalanine; poly(Ser), polyserine; poly(U), poly(uridylic acid); poly(A), poly(adenylic acid); anti-CPM IgG, rabbit polyclonal immunoglobulin G specific for CPM.

by MV^{2+} bound to rRNA in the immediate vicinity of the amino acid of Phe-tRNA in the peptidyl transferase center of the ribosome.

MATERIALS AND METHODS

Materials

3-(4-Maleimidophenyl)-7-diethylamino-4-methylcoumarin (CPM) and 3-(4-isothiocyanatophenyl)-7-diethylamino-4-methylcoumarin (CITC) were from Molecular Probes, Inc. (Eugene, OR). Purified yeast and *E. coli* tRNA^{Phe}, ethidium bromide, GTP, and methyl viologen (MV^{2+}) were from Sigma Chemical Co. (St. Louis, MO). [¹⁴C]Phenylalanine was purchased from ICN Radiochemicals, Inc. (Irvine, CA). Other chemicals were of reagent grade. The preparation of *E. coli* ribosomal subunits has been described previously (Odom et al., 1980).

Methods

Preparation of Fluorescent tRNA^{Phe} Derivatives. Yeast tRNA^{Phe} labeled at its 5' end with CITC (5'-CITC-tRNA^{Phe}) was prepared by a modification of the method of Mochalova and co-workers (Mochalova et al., 1982) as previously described (Odom et al., 1990). The 5'-labeled tRNA^{Phe} was aminoacylated and acetylated at the α -amino group to give 5'-CITC-NAcPhe-tRNA. The preparation of yeast Phe-tRNA which has been mercaptoacetylated at its α -amino group and subsequently labeled with CPM (to give CPM-SAcPhe-tRNA) is described in the same reference.

Aminoacylation and Acetylation of tRNA^{Phe}. Yeast tRNA^{Phe} (either 5'-CITC-tRNA^{Phe} or unlabeled tRNA^{Phe} for the preparation of CPM-SAcPhe-tRNA) was aminoacylated with the aminoacyl-tRNA synthetase fraction present in the 0.5 M KCl wash of rabbit reticulocyte ribosomes (Odom et al., 1990). The reaction mixture contained 50 mM Tris-HCl (pH 7.5), 20 mM magnesium acetate, 120 mM KCl, 2.5 mM dithioerythritol, 3.75 mM ATP, 60 μ M [¹⁴C]Phe (100 Ci/mol), 10 A₂₆₀ units of tRNA^{Phe}, and 40 μ g of protein from the synthetase fraction in a final volume of 1 mL. The mixtures were incubated for 30 min at 37 °C, phenol-extracted, and then ethanol-precipitated. All tRNA derivatives were purified by reversed-phase high-performance liquid chromatography (HPLC) (Odom et al., 1990).

Binding of tRNA to Ribosomes. Nonenzymatic binding of the tRNA^{Phe} derivatives to the P site of *E. coli* ribosomes was carried out by a procedure similar to that of Wurmbach and Nierhaus (1979). Briefly, the tRNA (10–30 pmol), poly-(U) (60 μ g), 50S ribosomal subunits (300 pmol), and 30S subunits (300 pmol) were mixed in 50 mM Tris-HCl (pH 7.5), 100 mM NH₄Cl, 15 mM magnesium acetate, and 5 mM 2-mercaptoethanol (buffer A) in a final volume of 0.6 mL. Binding was allowed to proceed for 15 min at 37 °C unless otherwise indicated. The coumarin moieties were also bound by anti-CPM IgG in buffer A. The anti-CPM IgG was prepared as described (Picking et al., 1992).

Fluorescence Measurements. A Model 8000 photon-counting spectrofluorometer from SLM-Aminco (Urbana, IL) was used for steady-state fluorescence determination as previously described (Rychlik et al., 1983). Spectra were measured at 1-nm intervals with a scanning rate of 1 s per wavelength increment. All samples had an absorbance of less than 0.01 at the excitation wavelength to avoid an inner filter effect. Unless otherwise indicated, all fluorescence measurements were taken in a volume of 0.6 mL and at a temperature of 20 °C. Steady-state anisotropy measurements were made

as described (Odom et al., 1984) with excitation of coumarin fluorescence at 385 nm and emission at 475 nm.

Fluorescence lifetime measurements were carried out at the Center for Fast Kinetics Research at The University of Texas at Austin. A mode-locked, synchronously pumped, cavity-dumped, frequency-doubled pyridine 1 dye laser with excitation at 385 nm and single-photon-counting detection (FWHM 70 ps) was used in a standard configuration as described (Harriman et al., 1992).

Quenching of Fluorescence with Methyl Viologen. Steady-state fluorescence was used to determine the Stern–Volmer quenching constants of MV^{2+} for ethidium bromide and coumarin dyes under a variety of conditions (Stern & Volmer, 1919). The fluorescence intensity of the sample was measured in the absence and presence of increasing concentrations of MV^{2+} . The degree of fluorescence quenching was plotted as F_0/F versus MV^{2+} concentration where F_0 is the fluorescence intensity in the absence of MV^{2+} and F is the intensity at a given concentration of MV^{2+} . The Stern–Volmer quenching constant (K_Q) is given by the slope of this plot. Where the slope deviated from linearity, the initial slope of the plot was used to determine K_Q .

In some cases, the Stern–Volmer plots curved upward which generally indicates the occurrence of both dynamic (diffusive) and static (nondiffusive) quenching processes (Lakowicz, 1983). These two separate quenching constants were determined by plotting the apparent $K_Q \{[(F_0/F) - 1]/[Q]\}$ at each MV^{2+} concentration versus the MV^{2+} concentration ($[Q]$) (Lakowicz, 1983). The slope of this plot gives the product of the diffusive quenching constant (K_D) and the static quenching constant (K_S). The y-axis intercept gives the sum of K_D and K_S . Each constant can be calculated from the quadratic equation $K^2 - KI + s = 0$, where I is the y-axis intercept and s is the slope. Once the two constants are known, it is possible to distinguish K_D from K_S by measuring fluorescence lifetime changes in response to the quenching agent. Lifetime measurements only reflect diffusive quenching and so can be used to calculate K_D . In some cases where only one constant is observed or one constant represents a predominant form of quenching, the main type of quenching can be determined as being diffusive or static by changing the temperature at which the quenching is measured. Diffusive quenching increases as the temperature increases due to the resulting increased rate of diffusion. Static quenching decreases as the temperature increases due to destabilization of complex formation.

When K_D is known, it is possible to determine the degree of protection a fluorophore is given from diffusional quenching by small molecules in the solvent. This is determined by dividing K_D by the fluorescence lifetime of the probe in the absence of quencher (K_D/τ_0) to give the bimolecular quenching rate constant (k_q) which is a direct measure of the rate at which the probe and quenching agent collide. This value decreases when a probe is shielded within a macromolecular complex, for instance, after binding of anti-coumarin IgG as indicated by the results given below.

RESULTS

Double-Stranded RNA Mediates the Methyl Viologen Quenching of Ethidium Bromide Fluorescence. Our initial objective was to compare MV^{2+} quenching of fluorescence from ethidium bromide (EB) intercalated into RNA with the well-documented results for EB in double-stranded DNA. EB intercalates into double-stranded DNA with a binding constant of $2.6 \times 10^6 \text{ M}^{-1}$ (Gauguin et al., 1978) with 0.4 EB/base pair at saturation (Fromherz & Reiger, 1986). Intercalation results

Table I: Methyl Viologen Quenching of Ethidium Bromide Fluorescence

conditions ^a	K_Q (M ⁻¹)
ethidium bromide alone (500 pmol)	9
+100 μ g of tRNA ^{Phe}	1.2×10^4
+60 μ g of poly(U)	9
+20 μ g of poly(A)	no quenching
+60 μ g of poly(U) and 20 μ g of poly(A)	3.7×10^4

^a All samples were in buffer A, and the Stern-Volmer quenching constant was measured with an excitation wavelength of 532 nm and an emission wavelength of 600 nm. Methyl viologen was added directly to the cuvettes used for fluorescence measurements. The intensity was corrected for the slight dilution which occurred upon adding MV²⁺.

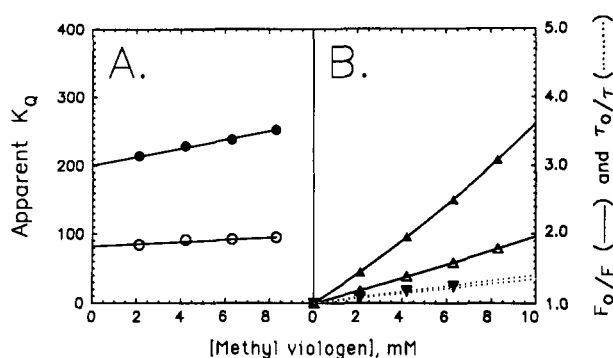


FIGURE 1: Determination of the quenching constants of methyl viologen for CPM-SAcPhe-tRNA fluorescence. In part A, the apparent quenching constants at various concentrations of MV²⁺ are plotted against the MV²⁺ concentration for free CPM-SAcPhe-tRNA (open circles) and CPM-SAcPhe-tRNA bound to poly(U)-programmed ribosomes (closed circles). The slope (s) is equal to the product of the diffusive (K_D) and static (K_S) quenching constants while the y -axis intercept (I) gives the sum of K_D and K_S . In part B, the dotted lines are the Stern-Volmer plots for the MV²⁺ quenching of the fluorescence lifetimes of free (open inverted triangles) and ribosome-bound (closed inverted triangles) CPM-SAcPhe-tRNA. The slopes of these plots are equal to the K_D of MV²⁺ for CPM-SAcPhe-tRNA fluorescence. The solid lines in panel B represent the Stern-Volmer plots of the steady-state fluorescence intensity of free (open triangles) and ribosome-bound (closed triangles) CPM-SAcPhe-tRNA. The quenching of free CPM-SAcPhe-tRNA (30 pmol) was measured in 0.6 mL of buffer A by adding increasing amounts of MV²⁺ (0–10 mM) directly to the cuvette used for fluorescence measurements. The resulting intensities were corrected for slight changes due to dilution upon adding MV²⁺. Bound CPM-SAcPhe-tRNA fluorescence quenching was similarly measured after incubation with 300 pmol of ribosomes and 60 μ g of poly(U).

in a 12-fold increase in the fluorescence lifetime of EB; however, the quenching of intercalated EB fluorescence by MV²⁺ is several thousandfold greater than that of EB in water (Fromherz & Reiger, 1986). This phenomenon has been attributed to the ability of MV²⁺ to form a mobile coat on the surface of DNA due to electrostatic attraction. This brings the intercalated fluorophore and quenching agent into close proximity. In other words, DNA has a mediating effect on the quenching reaction which occurs between MV²⁺ and EB (Atherton, 1988).

The ability of RNA to mediate MV²⁺ quenching of EB fluorescence was tested as shown in Table I. EB was quenched by MV²⁺ in the absence and presence of an 8-fold molar excess of *E. coli* tRNA^{Phe} in buffer A. As with DNA, the quenching increased over a thousandfold in the presence of tRNA^{Phe}, indicating that it was able to bring EB and MV²⁺ into reactive proximity. MV²⁺ quenching of EB fluorescence was even greater when measured in the absence of buffer and salts (data not shown) although this condition does not greatly alter the fluorescence of EB. This observation supports the conclusion of Atherton (1988) that MV²⁺ binding to nucleic

acid is primarily by electrostatic interaction with ionized phosphates along the backbone of the chain and that this interaction can be attenuated by the presence of competing cations.

Poly(U) or poly(A), single-stranded RNA, does not affect the quenching of EB fluorescence (Table I). Presumably, this is due to the lack of double-stranded structure in these RNAs and thus of EB intercalation, although they, like tRNA^{Phe}, are rich in negative charge and should still interact with MV²⁺. Indeed, when the two are mixed, the resulting double-stranded RNA affects the MV²⁺ quenching of EB fluorescence (Table I).

MV²⁺ Quenching of Ribosome-Bound CPM-SAcPhe-tRNA Fluorescence. We have previously observed that MV²⁺ quenching of the fluorescence from a coumarin probe attached to the α -amino group of synthetic alanyl-tRNAs is increased more than 2-fold upon binding to poly(U)-programmed *E. coli* ribosomes (Picking et al., 1992). A similar phenomenon was observed for a coumarin probe at the α -amino group of *E. coli* initiator methionyl-tRNA upon binding to MS2 RNA-programmed ribosomes (Picking et al., submitted for publication). These data indicated that the amino acid of ribosome-bound tRNA is not protected from interaction with small molecules in the solvent; however, these studies did not provide clear evidence on the degree of accessibility of the probes to collisional quenching by MV²⁺. To further investigate those findings, CPM-SAcPhe-tRNA fluorescence was quenched by MV²⁺ before and after binding to 70S ribosomes in the presence of poly(U). The quenching data were analyzed and are shown in Figure 1. The apparent $K_Q \{[(F_0/F) - 1]/[Q]\}$ was plotted versus the MV²⁺ concentration (Figure 1A). The slope and the y -axis intercept of this plot were used to calculate the diffusive and static quenching constants, K_D and K_S , respectively, for both free and ribosome-bound CPM-SAcPhe-tRNA; however, this plot does not indicate which of the two obtained values is K_D and which is K_S . K_D was determined by measuring the MV²⁺ quenching of the CPM-SAcPhe-tRNA fluorescence lifetime. In Figure 1B, Stern-Volmer plots are shown for both the steady-state fluorescence and the fluorescence lifetime quenching of CPM-SAcPhe-tRNA by MV²⁺. The Stern-Volmer plot of the fluorescence lifetime data (τ_0/τ versus [MV²⁺]) has a slope which is equal to K_D and which is similar to one of the constants calculated from the plot in Figure 1A. The remaining constant calculated from Figure 1A is K_S . An upward curvature in the Stern-Volmer plot of the steady-state fluorescence quenching by MV²⁺, for free and ribosome-bound CPM-SAcPhe-tRNA, indicates that both diffusive and static quenching processes are taking place (Figure 1B). Comparison with the results for the reaction product of CPM with 2-mercaptoethanol gives an indication of the effect of the tRNA portion of CPM-SAcPhe-tRNA on MV²⁺ quenching. For CPM-2-mercaptoethanol, K_D was 56 M⁻¹, and K_S was essentially zero (data not shown). It should be mentioned that the lifetimes given are average values. Usually a double-exponential fit to the data indicated that the decay curves were made up of at least two components. It appears likely that the emission may be comprised of a large number or continuous distribution of lifetimes, resulting in differences in the local environment of the fluorophore that are related to differences in conformation, solvation, mobility of the fluorophore, and other factors. Such distributions of fluorescence lifetimes have been demonstrated for fluorescence from tryptophan in proteins and analyzed in terms of the dynamics of the structure of the protein (Alcala et al., 1987). However, within the limits of the two-exponential

Table II: Methyl Viologen Quenching of CPM-SAcPhe-tRNA

position of CPM-SAcPhe-tRNA	K_D (M^{-1})	K_S (M^{-1})	τ_0 (ns)	k_q (K_D/τ_0) ($M^{-1} s^{-1}$)
free	45	51	2.6	1.7×10^{10}
ribosome P-site-bound	38	186	4.0	1.0×10^{10}
anti-CPM-bound	5	20	4.4	1.14×10^9

fit to the observed data, methyl viologen quenching was similar or identical for both lifetime components, suggesting that the use of the average lifetime value is an acceptable approximation for the purpose of our analysis.

The results of MV^{2+} quenching of CPM-SAcPhe-tRNA agree with previous observations that ribosome binding enhances the ability for MV^{2+} to quench the fluorescence from CPM-SAc-aminoacyl-tRNA (Table II). The data also indicate that the amount of quenching due to diffusional processes actually decreases from 45 to 38 M^{-1} upon ribosome binding. This is accompanied by an increase in fluorescence lifetime. The results indicate that ribosome binding only slightly reduces the amount of diffusion-limited collision which can occur between the probe and its quencher. This point is reflected by the decrease in the bimolecular quenching rate constant (k_q) upon ribosome binding (Table II).

The relatively small reduction in K_D and k_q demonstrates that the amino acid of Phe-tRNA, or at least the probe covalently linked to it, remains largely exposed to the solvent when the Phe-tRNA is bound into the ribosomal P site. These results can be compared directly with data for binding of the coumarin probe of free CPM-SAcPhe-tRNA by anti-CPM IgG (Table II) for which K_D is reduced to 5 M^{-1} and k_q to $1.1 \times 10^9 M^{-1} s^{-1}$. Considered with changes in the emission spectrum, quantum yield, fluorescence lifetime, and fluorescence anisotropy that occur upon interaction with IgG (data not shown), the results indicate that the probe is buried within a relatively hydrophobic pocket within the antibody where it is largely shielded from MV^{2+} in the solvent.

In contrast to diffusional quenching, the static quenching of CPM-SAcPhe-tRNA increases over 3-fold concomitant with ribosome binding (Table II). This suggests that ribosome binding results in placement of the probe into a region relatively rich in RNA that is accessible to MV^{2+} . RNA involvement is further suggested by the observation that quenching of CPM-SAcPhe-tRNA fluorescence by iodide (negatively charged) is almost completely abolished after ribosome binding (data not shown). The data appear to indicate that the ribosome holds the aminoacyl moiety of the tRNA tightly within the peptidyl transferase center while the rRNA of the peptidyl transferase center sequesters MV^{2+} in this region in much the same way that MV^{2+} is concentrated by double-stranded DNA. It is important to note here that static quenching in this case does not result from MV^{2+} forming a ground-state complex directly with the coumarin which would result in a perturbation of the coumarin absorbance spectrum (data not shown).

Effect of Nascent Peptide Length on Static Quenching. In previous studies, a relatively rapid decrease in K_Q was observed upon nascent peptide extension with coumarin at the amino terminus of the growing peptide (Picking et al., 1992). To measure the length of nascent peptide needed to exit the rRNA-rich region of the peptidyl transferase center, increasing lengths of poly(Phe) or poly(Ala) were synthesized with a CPM residue at their amino termini. Nascent peptide extension was stopped at specific times, and the incorporation of [^{14}C]phenylalanine or [^{14}C]alanine was measured. An average length of the nascent peptides was calculated based on the known number of active ribosomes in the sample (Picking et al., 1992). The

Table III: Methyl Viologen Quenching of CPM at the Amino Terminus of Nascent Polyphenylalanine and Polyalanine

av nascent peptide chain length (amino acid residues) ^a	K_Q (M^{-1})	K_D (M^{-1})	K_S (M^{-1})
polyphenylalanine			
1	224	38	186
4	154	30	124
13	127	11	116
polyalanine			
1	225	45	180
6	180	38	142
10	160	36	124
20	125	40	85

^a Nascent polypeptide chain length was determined by measuring the incorporation of [^{14}C]phenylalanine (25 Ci/mol) or [^{14}C]alanine (25 Ci/mol) and dividing by the concentration of active ribosomes as previously described (Picking et al., 1992). The nascent peptide-bearing ribosomes were isolated by gel filtration on Sephacryl S300 equilibrated with buffer A.

data for the quenching of poly(Phe) and poly(Ala) are shown in Table III. The K_D for poly(Phe) declines from 38 to 11 M^{-1} at a chain length of 13 residues whereas the K_D for poly(Ala) declines only slightly from 45 to 40 M^{-1} at a chain length of 20 residues. The corresponding values of K_S for poly(Phe) and poly(Ala) as they are extended are 186 to 116 M^{-1} and 180 to 85 M^{-1} , respectively. Poly(Phe) appears to collapse into an insoluble mass in or near the peptidyl transferase center as it is formed (Picking et al., 1991) which may lead to the observed changes in both K_D and K_S for this polypeptide; however, poly(Ala) is probably extended from the peptidyl transferase center as an α -helix as it is formed (Picking et al., 1992). The small decline in K_D as poly(Ala) is extended indicates that it is not significantly shielded by the ribosome from MV^{2+} in the solvent as might be anticipated if the N-terminal probe entered a tightly enclosed channel or tunnel from which MV^{2+} was excluded. The decline in K_S , however, suggests that the N-terminus moves away from the RNA-rich region as the peptide is extended. The distance for the 20-residue peptide would be 30 Å if the peptide was in the α -helical conformation.

Effect of Movement of the 5' End of tRNA on Static Quenching. We have previously reported that the 5' end of tRNA^{Phe} may move more than 20 Å toward ribosomal protein L1 during the peptidyl transferase reaction on *E. coli* ribosomes, whereas the nascent peptide, extended by a single amino acid upon peptidyl transfer, moves no more than a few angstroms (Odom et al., 1990). Movement of the deacylated tRNA following peptidyl transferase might be associated with a change in the local environment of that portion of the tRNA that would be reflected by MV^{2+} quenching. This possibility was investigated using tRNA^{Phe} with a coumarin covalently attached to its 5'-terminal phosphate (5'-CITC-tRNA^{Phe}) and its aminoacylated counterpart 5'-CITC-NACphe-tRNA^{Phe}. The aminoacylated and deacylated species were bound to poly-(U)-programmed ribosomes, and the MV^{2+} quenching of the fluorescence from each was measured and compared with their unbound counterparts.

The Stern-Volmer quenching constants for free 5'-CITC-tRNA^{Phe} and 5'-CITC-NACphe-tRNA are nearly the same (Table IV). When the deacylated derivative is bound to the ribosomal E site, only a small increase in K_Q is observed. Analysis of fluorescence lifetime data for 5'-CITC-tRNA^{Phe} indicates that ribosome binding results in a small increase in K_S which is largely offset by a small decrease in K_D so that total quenching is nearly the same for the free and E-site-

Table IV: Methyl Viologen Quenching of 5'-Labeled tRNA^{Phe} Derivatives

tRNA derivatives	position	K_Q (M ⁻¹)	K_D (M ⁻¹)	K_S (M ⁻¹)
5'-CITC-NAcPhe-tRNA ^{Phe}	free	91	16	75
	P-site-bound	122	12	110
5'-CITC-tRNA ^{Phe}	free	90	18	72
	E-site-bound	95	15	80

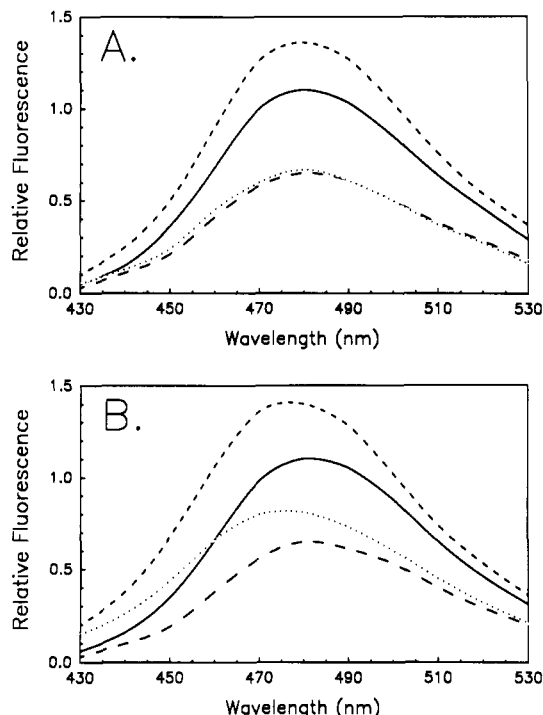


FIGURE 2: Fluorescence spectra of acylated and deacylated tRNA^{Phe} labeled at the 5' end with CITC. In part A, spectra are shown for free 5'-CITC-NAcPhe-tRNA before (solid line) and after (long dashed line) the addition of 8.3 mM MV²⁺. The emission spectra of ribosome-bound 5'-CITC-NAcPhe-tRNA are also shown before (short dashed line) and after (dotted line) the addition of 8.3 mM MV²⁺. In part B, emission spectra of free deacylated 5'-CITC-tRNA^{Phe} are shown before and after adding 8.3 mM MV²⁺ (solid and long dashed lines, respectively); the spectra of ribosome-bound 5'-CITC-tRNA^{Phe} are also shown before and after adding 8.3 mM MV²⁺ (short dashed and dotted lines, respectively). Excitation of fluorescence was at 385 nm. In each case, 10 pmol of tRNA was used; for binding, the samples were incubated with 60 µg of poly(U) and 300 pmol of ribosomes for 15 min at 37 °C in a final volume of 0.6 mL of buffer A.

bound tRNA (Table IV). Conversely, the K_S for MV²⁺ quenching of 5'-CITC-NAcPhe-tRNA^{Phe} increases significantly upon binding to the ribosomal P site; however, the increase is less than that observed for the coumarin probes attached at the α -amino group of Phe-tRNA. The K_D for 5'-CITC-NAcPhe-tRNA^{Phe} decreases from 16 to 12 M⁻¹ with ribosome binding, but this relatively large percentage change is offset by the much greater numerical increase in K_S (nearly 50%, Table IV). Binding of 5'-CITC-tRNA^{Phe}, the deacylated tRNA analogue, also results in a significant blue shift in the emission maximum of the coumarin probe (from 480 to 477 nm), suggesting entry into a relatively nonpolar environment (Figure 2). Conversely, 5'-CITC-NAcPhe-tRNA^{Phe} only shifts about 1 nm toward the blue, suggesting occupation of a site which is more polar than that occupied by its deacylated counterpart (Figure 2). These data may also suggest that the acceptor stem of acyl-tRNA in the P site is also in an RNA-rich region of the ribosome. The spectra shown in Figure 2

also reveal the degree of quenching (observed as a decrease in spectral intensity) given by 8.3 mM MV²⁺ for each free and ribosome-bound tRNA species. In no case did MV²⁺ cause a shift in the coumarin emission spectra which would indicate a change in the environment surrounding the probes upon MV²⁺ addition (Figure 2).

The observation that the aminoacylated 5'-labeled tRNA does not show as large an increase in MV²⁺ quenching upon ribosome binding as did the CPM-SAcPhe-tRNA may indicate that the 5' end of aminoacyl-tRNA lies further away from an rRNA-rich region of the peptidyl transferase center, while the 3' end lies directly within this region. A 20-Å movement of the 5' end of the tRNA appears to remove the 5' probe to a position in which MV²⁺ quenching of its fluorescence is not affected appreciably by rRNA.

DISCUSSION

The fluorescence lifetime data presented above show that the increase in quenching of fluorescence from CPM-SAc-aminoacyl-tRNA which occurs upon binding into the ribosomal P site is due entirely to an increase in static quenching with only a small decrease in collisional quenching. The latter results indicate that there is little shielding of the coumarin probe from MV²⁺ by the ribosome; that is, the probe is accessible to the solvent and to MV²⁺ ($M_r = 257$) dissolved in it even as the nascent peptide is extended from the peptidyl transferase center during its synthesis. In contrast to collisional quenching, however, static quenching increases markedly upon binding of the acyl-tRNA to the ribosome, indicating MV²⁺ is concentrated in the immediate vicinity of the probe by a mechanism that is independent of diffusion.

The extensive studies of MV²⁺ quenching of fluorescence from ethidium bromide intercalated into double-stranded DNA provide insight into the mechanism that may be involved in binding of MV²⁺. The primary factor in the interaction appears to be electrostatic attraction between the positively charged nitrogen atoms of the bipyridine and the ionized phosphate residues along the backbone of the DNA which forms what has been termed a "mobile coat" of MV²⁺ along the nucleic acid (Fromherz & Reiger, 1986). A similar phenomenon appears to occur with RNA judging from the quenching studies reported here. There is no evidence, however, for interaction of MV²⁺ with a protein. Indeed, anti-coumarin IgG or its Fab fragment sharply decreases MV²⁺ quenching of CPM-SAcPhe-tRNA (Table II). These considerations lead us to conclude that the observed increase in static quenching upon binding of CPM-SAcPhe-tRNA to the ribosome is due to MV²⁺ binding to RNA in the vicinity of the peptidyl transferase center of the ribosome. This probably involves some part of the 23S ribosomal RNA, probably within domain V (Noller, 1991). Although it cannot be excluded that binding of the aminoacyl-tRNA to the ribosome results in folding of the 3' end in such a way that the derivatized amino acid is brought into close proximity with the body of the tRNA, we believe this is very unlikely. The ribosome must position the tRNA in the peptidyl site in such a way that the ester bond linking the peptidyl moiety of the tRNA is accessible to and chemically reactive with the free amino group of the amino acid on the incoming aminoacyl-tRNA. Steric requirements, as considered by Rich (1974) and Spirin and Lim (1986), appear to strongly favor an extended conformation of the 3' end of the tRNA.

Consideration of the mechanism by which MV²⁺ quenching of fluorescence takes place provides an indication of the distance between rRNA-bound MV²⁺ and the fluorophore.

MV²⁺ quenches ethidium bromide fluorescence by an electron-transfer mechanism (Fromherz & Reiger, 1986; Atherton, 1988). The same mechanism, although less efficient, is the basis for MV²⁺ quenching of coumarin fluorescence (Jones et al., 1984). Electron-transfer reactions do not normally occur beyond a distance of 15 Å, and the edge to edge distance between donor and acceptor in most photoinduced electron-transfer reactions is usually on the order of 10 Å or less (Guarr et al., 1983). It follows that the rRNA region which results in increased quenching of CPM-SAcPhe-tRNA fluorescence upon ribosome binding is very near to or most likely within the peptidyl transferase center itself. Deacylation of AcPhe-tRNA results in rapid movement of the 5' end of tRNA^{Phe} out of the rRNA-rich area (see Table IV), and nascent peptide extension causes the N-terminus of polyphenylalanine and polyalanine to quickly exit the rRNA-rich area (see Table III). Taken together, all these findings indicate that the rRNA-rich region of the ribosome which causes enhanced quenching of CPM-SAcPhe-tRNA fluorescence is relatively compact and lies in the region where the aminoacyl portion of tRNA is held prior to formation of the new peptide bond. This may be the peptidyl transferase center itself.

These findings are consistent with previous results, mentioned in the introduction, specifically implicating the central loop of domain V of 23S RNA as being in close proximity to the peptidyl transferase center [reviewed by Noller (1991)]. Recently, Noller and his co-workers (Noller, 1992) reported that 50S ribosomal subunits from *Thermus aquaticus* retain most of their ability to form a peptide between fMet-tRNA and puromycin after the subunits had been incubated with proteinase K and extraction with phenol to remove 95% of the ribosomal protein. The results provide strong evidence that the peptidyl transferase function of 50S subunits is mediated by RNA. The results presented here appear to be entirely consistent with this conclusion.

ACKNOWLEDGMENT

We gratefully acknowledge the Center for Fast Kinetics Research (Austin, TX) and Stephen Atherton and Michael O'Neil for help with the time-resolved fluorescence work, Gisela Kramer for critical discussions, and Amy Whitworth for preparing the manuscript.

REFERENCES

- Alcala, J. R., Gratton, E., & Prendergast, F. G. (1987) *Biophys. J.* 51, 597–604.
- Atherton, S. (1988) in *Light in Biology and Medicine* (Douglas, R. H., Moan, J., & Dall'Acqua, F., Eds.) Vol. I, pp 71–84, Plenum Press, New York.
- Barta, A., Steiner, G., Brobins, J., Noller, H. F., & Kuechler, E. (1984) *Proc. Natl. Acad. Sci. U.S.A.* 81, 3607–3611.
- Cundliffe, E. (1986) in *Structure, Function, and Genetics of Ribosomes* (Hardesty, B., & Kramer, G., Eds.) pp 586–604, Springer-Verlag, New York.
- Czworkowski, J., Odom, O. W., & Hardesty, B. (1991) *Biochemistry* 30, 4822–4830.
- Fellner, P. (1974) in *Ribosomes* (Nomura, M., Tissieres, A., & Lengel, P., Eds.) pp 169–191, Cold Spring Harbor Laboratory, Cold Spring Harbor, NY.
- Fromherz, P., & Reiger, B. (1986) *J. Am. Chem. Soc.* 108, 5361–5362.
- Gaugain, B., Barbet, J., Capelle, N., Roques, B. P., & Le Pecq, J.-B. (1978) *Biochemistry* 17, 5078–5083.
- Guarr, T., McGuire, M., Strauch, S., & McLendon, G. (1983) *J. Am. Chem. Soc.* 105, 616–618.
- Hardesty, B., Odom, O. W., & Deng, H.-Y. (1986) in *Structure, Function, and Genetics of Ribosomes* (Hardesty, B., & Kramer, G., Eds.) pp 495–508, Springer-Verlag, New York.
- Hardesty, B., Odom, O. W., & Picking, W. D. (1992) *Biochimie* (in press).
- Harriman, A., Kubo, Y., & Sessler, J. L. (1992) *J. Am. Chem. Soc.* 114, 388–390.
- Jones, G., II, Griffin, S. F., Choi, C.-Y., & Bergmark, W. R. (1984) *J. Org. Chem.* 49, 2705–2708.
- Lakowicz, J. R. (1983) *Principles of Fluorescence Spectroscopy*, Plenum Press, New York.
- Moazed, D., & Noller, H. F. (1987a) *Nature* 327, 389–394.
- Moazed, D., & Noller, H. F. (1987b) *Biochimie* 69, 879–884.
- Moazed, D., & Noller, H. F. (1990) *J. Mol. Biol.* 211, 135–145.
- Moazed, D., Robertson, J. M., & Noller, H. F. (1988) *Nature (London)* 334, 362–364.
- Mochalova, L. V., Shatsky, I. N., & Bogdanov, A. A. (1982) *Bioorg. Khim.* 8, 239–242.
- Noller, H. F. (1991) *Annu. Rev. Biochem.* 60, 191–227.
- Noller, H. F., & Woese, C. R. (1981) *Science* 212, 403–411.
- Noller, H. F., Hoffarth, V., & Zimniak, L. (1992) *Science* 256, 1416–1419.
- Odom, O. W., Robbins, D. J., Lynch, J., Dottavio-Martin, D., Kramer, G., & Hardesty, B. (1980) *Biochemistry* 19, 5947–5954.
- Odom, O. W., Deng, H.-Y., Dabbs, E., & Hardesty, B. (1984) *Biochemistry* 23, 5069–5076.
- Odom, O. W., Deng, H.-Y., & Hardesty, B. (1988) *Methods Enzymol.* 164, 174–187.
- Odom, O. W., Picking, W. D., & Hardesty, B. (1990) *Biochemistry* 29, 10734–10744.
- Picking, W. D., Odom, O. W., Tsalkova, T., Serdyuk, I., & Hardesty, B. (1991) *J. Biol. Chem.* 266, 1534–1542.
- Picking, W. D., Picking, W. L., Odom, O. W., & Hardesty, B. (1992) *Biochemistry* 31, 2368–2375.
- Rappoport, S., & Lapidot, Y. (1974) *Methods Enzymol.* 29, 685–688.
- Raue, H. A., Musters, W., Rutgers, C. A., Van't Riet, J., & Planta, R. J. (1990) in *The Ribosomes: Structure, Function, and Evolution* (Hill, W. E., Dahlberg, A., Garrett, R. A., Moore, P. B., Schlessinger, D., & Warner, J. R., Eds.) pp 217–235, American Society for Microbiology, Washington, D. C.
- Rich, A. (1974) in *Ribosomes* (Nomura, M., Tissieres, A., & Lengyel, P., Eds.) pp 871–884, Cold Spring Harbor Laboratory, Cold Spring Harbor, NY.
- Rychlik, W., Odom, O. W., & Hardesty, B. (1983) *Biochemistry* 22, 85–93.
- Schwartz, I., & Ofengand, J. (1978) *Biochemistry* 17, 2525–2530.
- Shine, J., & Dalgarno, L. (1974) *Proc. Natl. Acad. Sci. U.S.A.* 71, 1342–1346.
- Skold, S. K. (1983) *Nucleic Acids Res.* 11, 4923–4932.
- Spirin, A. S., & Lim, V. I. (1986) in *Structure, Function, and Genetics of Ribosomes* (Hardesty, B., & Kramer, G., Eds.) pp 556–572, Springer-Verlag, New York.
- Stern, D., & Volmer, M. (1919) *Phys. Z.* 20, 183–188.
- Thompson, J., Schmidt, F., & Cundliffe, E. (1982) *J. Biol. Chem.* 257, 7915–7917.
- Wurmbach, P., & Nierhaus, K. H. (1979) *Proc. Natl. Acad. Sci. U.S.A.* 76, 2143–2147.

Registry No. Peptidyl transferase, 9059-29-4.